

# The calculated attenuated total reflection (ATR) for analyzing surface plasmon polaritons

Vincensius Gunawan

Physics Department, Faculty of Sciences and Mathematics, Diponegoro University, Jl. Prof. Soedarto, Tembalang, Semarang, Indonesia

## Abstract

The electromagnetic waves propagate in the interface between metal and dielectric can be simply called surface plasmon polariton. The surface plasmon polaritons were produced by the coupling of incoming electromagnetic waves and collective vibrations of free charges on metal surface. The generation of surface polaritons may be done using attenuated total reflection (ATR) method which was based on total internal reflection. The method can be performed numerically by analyzing reflections on each involved interfaces. The generated surface plasmon polaritons were represented by the appearance of the dip in the ATR spectroscopy. In this paper, we presented the ATR spectroscopy for surface plasmon polaritons generated on gold-castor oil interface. The results showed the predicted dispersion relation from calculated ATR of the surface plasmons polaritons were in good agreement with the dispersion relation from the theory.

**Keyword:** dispersion relation, plasmon polaritons, attenuated total reflection

## Introduction

Surface plasmon polaritons (SPP) were electromagnetic waves, which propagate along the interface between dielectric and metal. Here, metal is an active medium, which provides collective free electron vibrations while dielectric is a passive medium that maintain electric fields at the interface. The features of SPP had already reported in the early of 20th century (Wood, 1968; Garnet, 1904; Mie, 1908). Since then, the SPP have received high attention due to its potential application such as: biosensors using plasmonic metamaterials (Kabashin et al., 2010), data storage capable to store data in the scale of terabits cells using plasmonic near-field transducers (O'Connor et al., 2009), wave-guides by fabricating patterned structure of metals and silicon (Nagpal et al., 2009) and also solar cells in increasing absorption by grooving Si thin film (Ferry et al., 2008).

There were several methods to excite SPP, such as gratings method, diffraction of roughness surface (Zayats et al., 2003; Zhang et al., 2012) and attenuated total reflection (ATR) (Otto, 1968; Kretschmann et al., 1968). The concept of ATR method based on the total internal reflection. Hence, it is required a high index prism to produce evanescent waves which then excite SPP at the interface between dielectric and metal. The ATR have used to study the properties of polaritons in several materials both experimentally and numerically. Analysis of both surface and bulk polaritons in dielectrics were analyzed using ATR method (Borstel et al., 1974). Surface phonon polaritons on the surface of dielectric GaN were studied using ATR (Torii et al., 2000). The ATR method is applied in explaining magnon polaritons in magnetic FeF<sub>2</sub> (Jensen et al., 1995; Jensen et al., 1997). The reciprocal property of surface polaritons on the surface of semi-infinite multiferroics was shown in ATR spectroscopy (Gunawan et al., 2011). The existence of surface polaritons on multiferroic film were also predicted numerically using calculated ATR (Gunawan et al., 2017; Gunawan et al., 2021).

The ATR spectroscopy was obtained by measuring the ATR reflectance. The sharp dip in ATR spectroscopy represents the existence of surface polaritons. The dip's frequency and the related vector propagation lead to the point at dispersion relation curves. Then, if we vary the vector propagation of initial electromagnetic waves by changing the initial angle, the set of related surface modes frequency can be obtained. Hence, the part of surface polariton's dispersion relation can be constructed using the resulted data. The dispersion

relation was important parameter since it reflected the properties of polaritons. The analysis of dispersion relation is one way to study polaritons, especially the surface modes.

In this present report, we predict the dispersion relation by analyzing the calculated ATR. Here, we focus on the surface plasmon polaritons which is generated at the interface metals and liquid dielectrics. In numerical process, we used parameters appropriate for gold to represent metals while parameters for castor oils were used to illustrated liquid dielectric.

### The method and formulation

In this numerical analysis, we used high index prism in the top of liquid dielectric while metal was placed below as illustrated in Figure 1. Here, we set all of surfaces at the x-y plane. Incoming electromagnetic waves with initial angle  $\theta$  was propagating into the prism. Then, the total internal reflection occurred at the bottom of the prism creating evanescent waves that might travel to the interface between dielectric and metal. When the frequency of incoming waves near the frequency of surface plasmons, the evanescent wave can excite those plasmons lead to the generation of surface plasmon polaritons (SPP) that propagate along the interface, parallel to the  $\hat{x}$  axis. In Figure 1. The red arrow represent SPP.

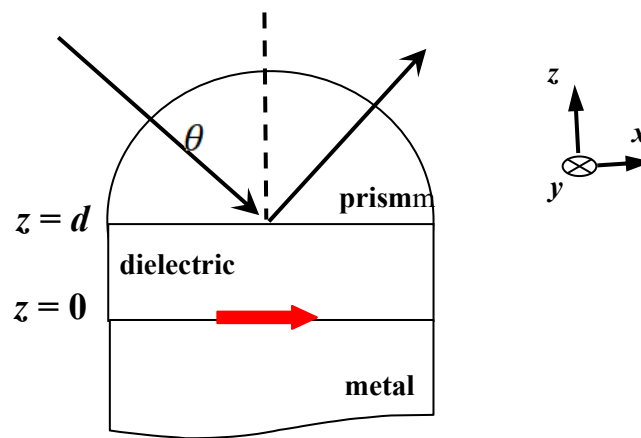


**Figure 1.** Geometry of the ATR. Dielectric and metal were placed under high index prism. The total internal reflection happened when incoming waves with initial angle  $\theta$  travelled into the bottom of the prism. The obtained evanescent waves propagated to the interface between dielectric and medium result in the generation of SPP that travel along the interface

The calculation of ATR spectroscopy was performed by firstly determine the involved field in each region. Since in this analysis we focused on the transversal magnetic (TM) modes where the magnetic component of electromagnetic waves was perpendicular to the plane of incidence, then we may determine the magnetic component as

$$\vec{H} = \hat{y} H_m \exp(\beta z) e^{i(k_x x - \omega t)} \quad \text{for } z < 0, \quad (1)$$

$$\vec{H} = \hat{y} [H_d \exp(\beta_0 z) + \tilde{H}_d \exp(-\beta_0 z)] e^{i(k_x x - \omega t)} \quad \text{for } 0 < z < d \quad (2)$$

and

$$\vec{H} = \hat{y} [H_p \exp(-ik_z z) + \tilde{H}_p \exp(ik_z z)] e^{i(k_x x - \omega t)} \quad \text{for } d < z. \quad (3)$$

Here, the attenuation constant was given as  $\beta = [k_x^2 - \epsilon_m \frac{\omega^2}{c^2}]^{1/2}$  where  $\epsilon_m$  represented dielectric constant for metal. The parameter  $\beta_0 = [k_x^2 - \epsilon_d \frac{\omega^2}{c^2}]^{1/2}$  represented attenuation constant with  $\epsilon_d$  was permittivity for dielectric. Using Ampere's law in Maxwell's equation,  $\nabla \times \vec{H} = \frac{1}{c} \frac{\partial \vec{D}}{\partial t}$ , we can derive the normal component of displacement fields as

$$D_z = \frac{-ck_x}{\omega} H_m \exp(\beta z) e^{i(k_x x - \omega t)} \quad \text{for } z < 0 \quad (4)$$

$$D_z = \frac{-ck_x}{\omega} [H_0 \exp(\beta_0 z) + \tilde{H}_0 \exp(-\beta_0 z)] e^{i(k_x x - \omega t)} \quad \text{for } 0 < z < d \quad (5) \text{ and}$$

$$D_z = \frac{-ck_x}{\omega} [H_p \exp(ik_z z) + \tilde{H}_p \exp(ik_z z)] e^{i(k_x x - \omega t)}, \quad \text{for } d < z \quad (6)$$

Tangential components of electric field can be derived using tangential components of  $\vec{D}$  field and consecutive equation,  $\vec{D} = \epsilon \vec{E}$ , lead to the form

$$E_x = \frac{-ic\beta}{\epsilon_m \omega} H_m \exp(\beta z) e^{i(k_x x - \omega t)} \quad \text{for } z < 0 \quad (7)$$

$$E_x = \frac{-ic\beta_0}{\epsilon_d \omega} [H_0 \exp(\beta_0 z) - \tilde{H}_0 \exp(-\beta_0 z)] e^{i(k_x x - \omega t)} \quad \text{for } 0 < z < d \quad (8)$$

$$E_x = \frac{c}{\epsilon_p \omega} [-H_p \exp(-ik_z z) + \tilde{H}_p \exp(ik_z z)] e^{i(k_x x - \omega t)} \quad \text{for } d < z. \quad (9)$$

The next step was analyzing the continuity of the fields at the interfaces. Continuity of the fields at  $z = 0$  leads to the reflectivity at the interface between dielectric and metal as

$$r = \frac{\epsilon_m \beta_0 - \epsilon_d \beta}{\epsilon_m \beta_0 + \epsilon_d \beta}, \quad (10)$$

while the continuity of fields at  $z = d$ , result in the relation as

$$r_d = \frac{[\epsilon_d k_y (1 + r e^{-2\beta_0 d}) - i \epsilon_p \beta_0 (1 - r e^{-2\beta_0 d})]}{[\epsilon_d k_y (1 + r e^{-2\beta_0 d}) + i \epsilon_p \beta_0 (1 - r e^{-2\beta_0 d})]} \quad (11)$$

Then, the ATR reflectivity was determined by

$$R = (r_d r_d^*)^{1/2}. \quad (12)$$

The calculated ATR spectroscopy was obtained by scanning frequency at the certain interval using Eq.(12).

## Results and Discussion

In this report, we used plasma frequency of metal,  $\omega_p = 5.8$  eV that is equivalent to  $\omega_p = 2.94 \times 10^5 \text{ cm}^{-1}$  appropriate for gold. The dielectric constant for gold was calculated using relation,  $\epsilon_m = \left(1 - \frac{\omega_p^2}{\omega^2}\right)$ . We also used the dielectric constant,  $\epsilon_d = 14.78$  representing castor oil as liquid dielectric. Permittivity for high index prism was  $\epsilon_p = 32.5$  representing thallium halogenide (KRS-5) crystal. The calculated ATR spectroscopy of surface plasmon polariton generated at the interface between gold and liquid dielectric (castor oil) was presented in figure 2a, while intersection between ATR line and dispersion relation was illustrated in figure 2b.

The calculated ATR spectroscopy showed the generation of the SPP by the existence of the dip in the spectroscopy curve. In our calculated ATR spectroscopy using castor oil-gold as at figure 2a, we obtained a dip around frequency  $0.4 \times 10^5 \text{ cm}^{-1}$  which showed the probability to generate SPP. Here, we used the dielectric thickness  $0.35 \text{ cm}$  and damping  $0.12 \times 10^5 \text{ cm}$ . The trend of the calculated ATR in this paper (figure 2a) was similar to the trend of the ATR spectroscopy from the previous studies (Jensen, 1997; Gunawan, 2021).

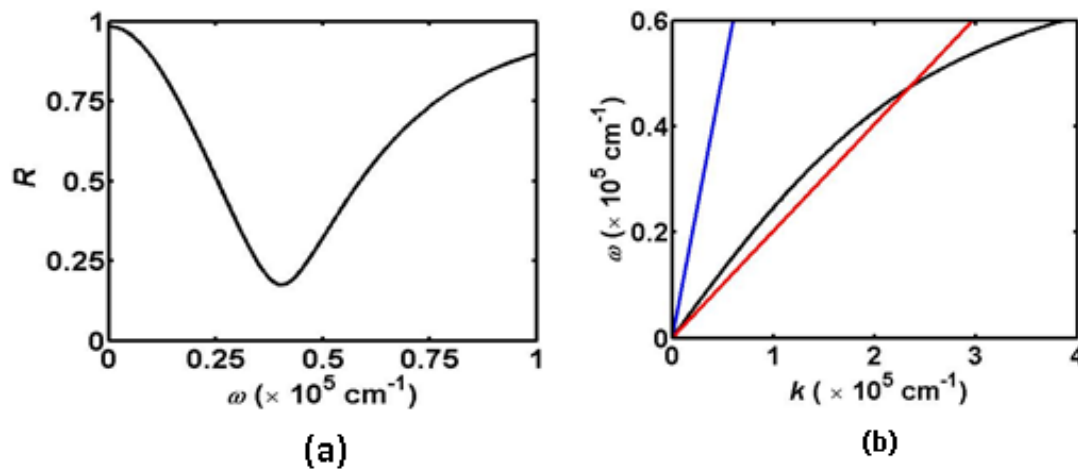


**Figure 2.** The calculated ATR spectroscopy and ATR line. In (a), the curve illustrated the dip in ATR spectroscopy. In (b), the figure showed the cross section between ATR line (red line) and

dispersion relation's curve (black curve). The blue line in figure 1b represented the vacuum light line.

The dip in ATR spectroscopy was related to the intersection between ATR line and dispersion relation curve (see figure 2b). It can be seen that the frequency of the dip at figure 2a was relatively similar to the frequency of the intersection at figure 2b. In those two figures, the value of propagation vector  $\vec{k}$  in ATR was similar to the propagation vector at the intersection in figure 2b. Then, by analyzing the ATR spectroscopy at the various values of propagation number, we may predict the dispersion relation curve. In ATR spectroscopy, the ATR line can be varied by adjusting the initial angle through the relation  $k_x = \sqrt{\epsilon_p} \frac{\omega}{c} \sin \theta$ . The results of our calculation for various initial angle were presented in figure 3 below.

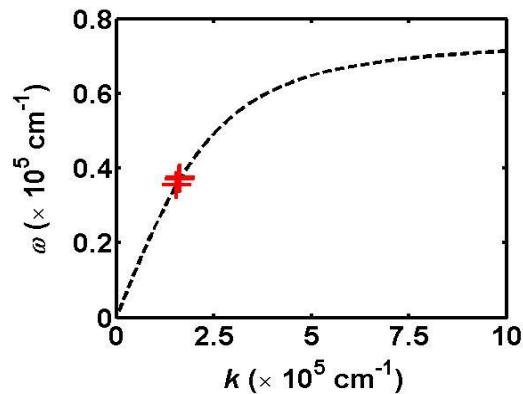


**Figure 3.** The Dispersion relation of SPP. The red cross markers were the data from ATR spectroscopy while the black dashed line represented the dispersion relation from the theory.

The figure 3 showed the good agreement between the results from calculated ATR, which were represented by red cross markers, with the dispersion relation from the theory, which was drawn using dashed line with the formulation was  $k_x = \frac{\omega}{c} \sqrt{\frac{\epsilon_d \epsilon_p}{\epsilon_d + \epsilon_p}}$ . Since critical angle for total internal reflection in KRS-5 crystal and castor oil system relatively high, around  $43^\circ$ , then we only vary the initial angle from around  $50^\circ$  to  $80^\circ$ . Hence, there were only little part of dispersion relation that could be constructed using calculated ATR. The increase of initial angle interval might be achieved by reducing the critical angle. Changing the castor oil by other dielectric materials with the low dielectric constant will decrease the critical angle. Then, the better part of dispersion relation may be obtained. However, the values of dielectric constant from other vegetable oils such as crude palm oils (CPO), coconut oils and sunflower oils were high. Hence, the calculated ATR spectroscopy can only predict the existence of surface plasmon polaritons generated in the vegetable oil-metal interface.

## Conclusion

The numerical ATR can predict the generation of surface plasmon polaritons in vegetable oil-metal interface. However, since the value of dielectric constant of vegetable oil is high, the results from calculated ATR can only construct little part of dispersion relation

## Acknowledgment

We highly acknowledge Physics Department, Faculty of Sciences and Mathematics, Diponegoro University for the support of this work

## References

1. Borstel, G., Falge, H. J. and Otto, A., Solid State Physics: Springer Tracts in Modern Physics Vol. 4, Ed. By G. Hohler (Springer-Verlag Berlin Heidelberg GmbH, New York, 1974) 107-148.
2. Ferry, V. E., Sweatlock, L. A., Pacifici, D. and Atwater, H. A., , "Plasmonic nanostructure design for efficient light coupling into solar cells", Nano Letters **8** 4391, 2008. (doi: 10.1021/nl8022548).
3. Garnet, J. C. M., "Colours in metal glasses and in metallic films", Phil. Trans. R. Soc. Lond. **203**,

- 385,1904 (doi 10.1098/rsta.1904.0024)
4. Gunawan, V. and Stamps, R. L., "Surface and bulk polaritons in PML-type magnetoelectric multiferroic with canted spins: TE and TM polarisation", *J. Phys: Condens. Matter* 23, 105901, 2011. (doi:10.1088/0953-8984/23/10/105901/meta).
  5. Gunawan, V. and Widiyandari, H., "Polaritons in magnetoelectric multiferroics films: Switching magnon polaritons using an electric field", *Ferroelectrics* 510, 16-26, 2017. (doi: 10.1080/00150193.2017.1326286).
  6. Gunawan, V. and Umiati, N. A. K., "Phonon polaritons in magnetoelectric multiferroics film: the possibility to drive surface modes using magnetic field", *Can. J. Phys.* 99, 150-158, 2021. (doi:10.1139/cjp-2020-0081).
  7. Jensen, M. R. F., Parker, T. J., Abraha K. and Tilley, D. R., "Experimental observation of magnetic surface polaritons in FeF<sub>2</sub> by attenuated total reflection", *Phys. Rev. Lett.* **75**, 3756, 1995. (doi: 10.1103/PhysRevLett.75.3756).
  8. Jensen, M. R. F., Feiven, S. A., Parker, T. J. and Camley, R. E., "Experimental determination of magnetic polariton dispersion curves in FeF<sub>2</sub>", *J. Phys.: Condens Matter* 9, 7223, 1997. (doi: 10.1103/PhysRevB.55.2745).
  9. Kabashin, A. V., Evans, P., Pastkovsky, S., Hendren, W., Wurtz, G. A., Atkinson, R., Pollard, R., Podolsky, V. A., and Zayats, A. V., "Plasmonic nanorod metamaterials for biosensing" *Nat. Mat.* **8**, 867, 2010. (doi: 10.1038/nmat2546).
  10. Kretschmann, E. and Raether, H., "Radiative decay of non radiative surface plasmon excited by light", *Z. Naturf. A* 23 2135, 1968. (doi: 10.1515/zna-1968-1247).
  11. Mie, G., "Contributions on the optics of turbid media, particularly colloidal metal solutions", *Ann. Phys.* **25**, 377,1908. (doi: 10.1002/andp.19083300302).
  12. Nagpal, P., Lindquist, N. C., Oh, S. H. and Norris D. C., "Ultrasmooth patterned metals for plasmonic metamaterials", *Science* **325**, 594, 2009, (doi: 10.1126/science 1174655).
  13. O'Connor, D. and Zayats, A. V., "Data storage: The third plasmonic revolution", *Nat Nanotechnol* **5** 482, 2009. (doi:10.1038/nnano.2010.137)
  14. Otto, A., "Excitation of nonradiative surface plasma waves by the method of frustated total reflection", *Z. Phys.* 216 1530, 1968. (doi: 10.1007/BF01391532).
  15. Torii, K, Koga, T., Sota, T., Azuhata, T., Chichibu, S. F. and Nakamura, S., "An attenuated total reflection study on the surface phonon polariton in GaN", *J. Phys.:Condens Matter* 12, 7041, 2000. (doi: 10.1088/0953-8984/12/31/305).
  16. Wood, R. W., "On a remarkable case of uneven distribution of light in a diffraction grating spectrum", *Phil. Mag.***4**, 396, 1902. (doi: 10.1080/14786440209462857)
  17. Zayats, A. V. and Smolyaninov, I. I., "Near-field photonics: surface plasmon polaritons and localized surface plasmons", *J. Opt. A.: Pure Appl. Opt* 5 S16 (2003). (doi: 10.1088/1464-4258/5/4/353).
  18. Zhang, J., Zhang, L. and Xu, W., "Surface plasmon polaritons: physics and applications", *J. Phys. D.: Appl. Phys.* 48 113001, 2012. (doi: 10.1088/0022-3727/45/11/113001).